FULL PAPER

Highly Luminescent ZnO Quantum Dots Made in a Nonthermal Plasma

Patrick Felbier, Jihua Yang, Jens Theis, Richard William Liptak, Andrew Wagner, Axel Lorke, Gerd Bacher, and Uwe Kortshagen**

Nonthermal plasmas allow the preparation of ligand-free quantum dots combining high production rates with superior crystalline quality and luminescence properties. Here, ZnO quantum dots are produced in a radiofrequency capacitively-coupled plasma, exhibiting size dependent photoluminescent quantum yields up to 60% after air exposure—the highest reported to date for any compound semiconductor quantum dots prepared in the gas phase. Systematic studies indicate the importance of the surface for the observed luminescence behavior. The high luminescent quantum yields in the visible range of the spectrum and the ligand-free, scalable synthesis make these quantum dots good candidates for light emitting applications.

1. Introduction

ZnO quantum dots are attractive candidates for a variety of applications, such as solar cells and light-emitting devices[1–5] (LEDs) or bio-imaging.[6–8] The interest in ZnO as the active material in nanocrystal LEDs arises from its superior exciton stability at room temperature, with a binding energy of 60 meV. In addition, ZnO is capable of emitting light both in the ultraviolet (UV) through near bandgap emission and in the visible through defect and surface state mediated emission.[6,8,9] Because the Bohr exciton radius of bulk ZnO is 2.34 nm,[10] nanometer-sized ZnO nanocrystals exhibit quantum confinement,[11–15] which may allow tuning of emission wavelengths via the quantum dot size.

P. Felbier, Prof. G. Bacher
Werkstoffe der Elektrotechnik and CENIDE
University of Duisburg-Essen
47057, Duisburg, Germany
E-mail: gerd.bacher@uni-due.de
Dr. J. Yang, A. Wagner, Prof. U. Kortshagen
Department of Mechanical Engineering
University of Minnesota Minneapolis
MN, 55455, USA
E-mail: kortshagen@umn.edu
J. Theis, Prof. A. Lorke
Fakultät für Physik and CENIDE
University of Duisburg-Essen
47048, Duisburg, Germany
R. W. Liptak
Department of Electrical and Computer Engineering
University of Minnesota Minneapolis
MN, 55455, USA

DOI: 10.1002/adfm.201303449

A critical issue for optical applications of ZnO quantum dots is the luminescent quantum yield. Previous reports based on chemical sol-gel processes mentioned luminescent ZnO quantum dots with quantum yields as high as ≈26%.[8] Tuneable emission in the blue to yellow range of the spectrum with quantum yields as high as 61% was reported for ZnO quantum dots synthesized by LiOH-mediated growth and a post-crystallization surface capping.[6] Quantum yields up to 76% in the blue were achieved by complexing the ZnO surfaces with oleic acid;[16] however, the quantum yield decayed over times of a few days. Aside from the crystal quality and post-processing, it was demonstrated that the quantum dot diameter is an important factor for quantum yield with the highest quantum yields having been observed for nanocrystal diameters of only a few nm.[11] In this size range, the large surface to volume ratio enhances the importance of surface states that are presumed to play a central role for visible emission.[17] As surface states interact with the environment, it is important to consider the ambient when comparing and analyzing luminescence properties of ZnO quantum dots.

The high quantum yields achievable with ZnO quantum dots demonstrate that they may be an interesting alternative to liquid phase synthesized chalcogenide semiconductor quantum dots. Different from those materials, the inherent nontoxicity of ZnO and its strong defect luminescence in the green suggest applications in bio-imaging. The ligand-free synthesis in the gas phase may be an advantage for optoelectronic device applications, as it obviates the need for ligand removal or replacement schemes typically required to achieve good electronic transport in nanocrystal films. Among gas phase routes to synthesize ZnO quantum dots are flame pyrolysis,[18,19] hot-wall reactors,[20,21] microwave plasmas,[19] or a combination of the latter two.[21] To date, the smallest ZnO nanoparticles produced in the gas phase were between 4–6 nm in diameter and were synthesized in a microwave plasma.[19] However, there are no reports on quantum yields of ZnO nanoparticles made in the gas phase up to now.

Here we report on the synthesis and photoluminescent properties of ZnO quantum dots made in a scalable nonthermal plasma process. Gas phase synthesis is extremely fast (a few milliseconds to tens of milliseconds),[22] continuous (liquid phase processes are often run in batch form and the characteristics of QDs from different batches may vary),[23]

largely scalable (up to kg or even tons) and ligand-free, which makes this synthesis route highly interesting for large scale applications, for example, in light emitting devices. We obtain size-controlled ZnO quantum dots with efficient luminescence without any further surface chemical treatment. As our quantum dots are ligand-free, we are in a position to discuss, for instance, the role of surface OH groups in the visible emission mechanism under different atmospheric conditions much clearer than in case of usual liquid-phase approaches. The ZnO quantum dots synthesized here are smaller than in previous reports on gas phase synthesis and range between 2.1–3.4 nm. They exhibit a clear blue-shift in light emission with decreasing size, indicating quantum confinement. The luminescent quantum yield is largest for the smallest quantum dots of 2.1 nm and reaches 60%. Fourier transform infrared spectroscopy (FTIR) and photoluminescence (PL) support the importance of adsorbed surface groups for efficient visible luminescence.

2. Quantum Dot Synthesis

The ZnO quantum dots were synthesized in a nonthermal, low pressure flow-through reactor equipped with a 13.56 MHz radio-frequency plasma source. Diethylzinc (DEZ) and molecular oxygen (O_2) were the precursor materials, using argon (Ar) as the background gas. One challenge arises from using these precursors: they will react with each other spontaneously, resulting in uncontrolled deposition of a low-quality film on the reactor walls. To prevent this, both precursor species have to be injected separately into the plasma for dissociation before they mix and finally react. **Figure 1** shows a sketch of the newly designed reactor that solves this challenge. Rather than mixing the precursors in a gas line prior to their entry into the plasma, the DEZ vapor was injected through an inlet tube that extended into the main reactor chamber, while a mixture of O_2 and Ar was passed through a sidearm tube and filled the space around the upper injection line. The ring electrodes were placed such that plasma initiated about 1cm above the end of the top line and the discharge extended downstream in order to dissociate and charge the DEZ and O_2 molecules individually before they mixed in the main reactor chamber. The nominal applied plasma power read at a power meter was 100 W, though the power actually coupled to the plasma is much lower. DEZ vapor was injected with a flow rate of 6 standard cubic cm per minute (sccm), controlled using a needle valve. The O_2 flow rate was 3 sccm, and the Ar flow rate was 40 sccm. ZnO quantum dots were formed in the plasma and collected at the reactor exhaust on stainless steel mesh filters. The size of the resulting quantum dots was changed by varying their residence time in the plasma. This was controlled by adjusting the pressure in the plasma reactor over the range of 0.5–1.3 Torr (66–200 Pa) using an electronic butterfly valve to throttle the vacuum pump. An additional reactor with a reduced diameter was used for making the smallest particles, using similar gas flow rates and plasma power.

The crystallinity of the ZnO quantum dots was studied using X-ray diffraction (XRD). The diffraction patterns correspond closely to the pattern for wurtzite ZnO. From the Scherrer equation,[24] which correlates the peak broadening with the quantum dot size, we calculated crystallite diameters of 3.4 nm, 3.0 nm and 2.4 nm for the samples made in the larger-diameter reactor at 1.3 Torr, 1.0 Torr, and 0.5 Torr, respectively, and 2.1 nm for the quantum dots prepared in the smaller-diameter tube. **Figure 2** shows the XRD pattern from the 3.4 nm ZnO quantum dots. The crystallinity of the ZnO quantum dots is also demonstrated by the periodic electron diffraction seen in the high-resolution transmission electron microscopy (HRTEM) image (inset of Figure 2). Note that these ZnO quantum dots are among the smallest synthesized by a gas phase approach reported in literature thus far.

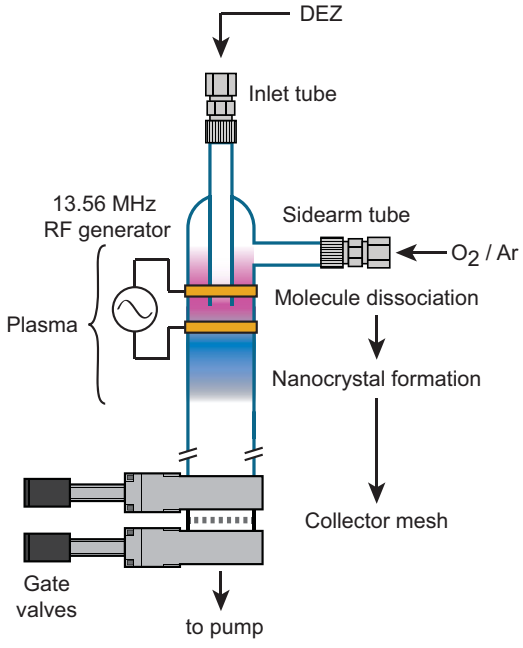

Figure 1. Sketch of plasma reactor chamber.

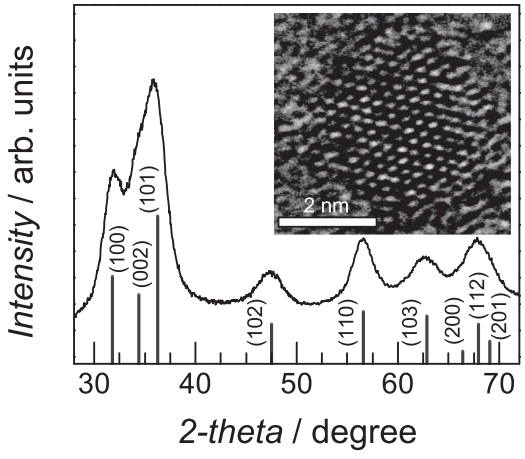

Figure 2. X-ray diffraction pattern of the ZnO quantum dots with a diameter of 3.4 nm. Vertical lines indicate the diffraction peak position and intensity of bulk wurtzite ZnO. The inset shows a HRTEM image of the ZnO quantum dot.

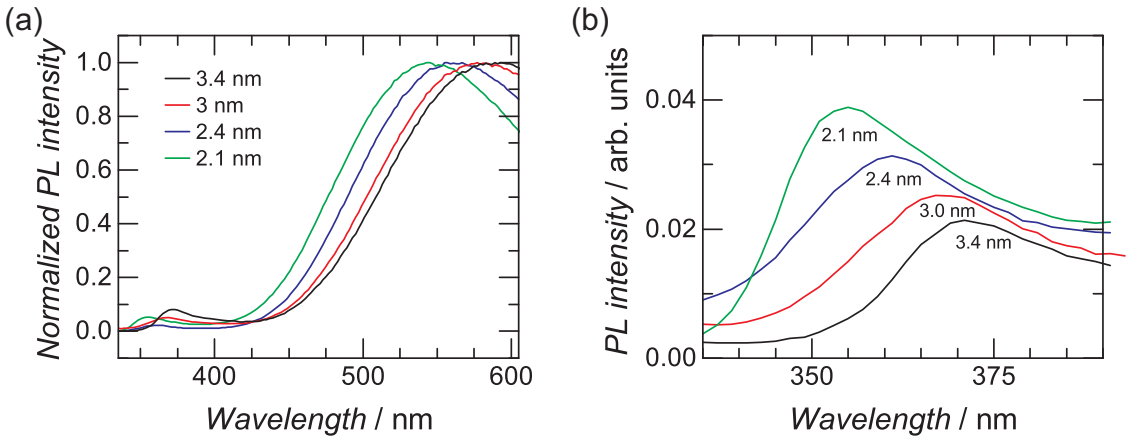

Figure 3. a) Normalized photoluminescence (PL) spectra of the ZnO quantum dots with diameters between 2.1 nm and 3.4 nm. b) Near-bandgap exciton emission in more detail for 2.1 nm to 3.4 nm quantum dots.

3. Luminescence Properties

The normalized photoluminescence (PL) spectra of the ZnO quantum dots dispersed in ethanol are depicted in **Figure 3**a. The spectra were measured after the particle dispersions were exposed to ambient air for 12 hours. The majority of the light emission is spread over the visible spectral range with the maximum intensity in the green/yellow region, from 550 to 590 nm, with some contribution in the UV region due to near-bandgap exciton emission. The yellow/green emission component is likely defect emission due to surface states. We observe a blue shift of the emission maxima with decreasing size, for both the visible (Figure 3a) and the UV (see Figure 3b) emission. The near-bandgap emission shifts from 371 nm for the largest quantum dots to 355 nm for the smallest ones due to quantum confinement (see Figure 3b). Note that the size dependent bandgap shift is much less than expected by a simple effective mass model. For example, for a particle size of 3.4 nm, we observe a PL maximum emission at 371 nm, while the effective mass model predicts 305 nm. This strong discrepancy is well known for ZnO and widely discussed in literature.[25–30] Some of the main reasons discussed in literature are: Stokes shift between absorption and emission peak due to different fine structure states involved,[27,28] or due to phonon interaction,[28] leakage of the carrier wave function to surface states (i.e., a finite well depth height),[29] or Stark shift due to a strong electric field due to surface charges.[30]

Photoluminescence blue shifting with decreasing quantum dot size from 589 nm for 3.4 nm quantum dots to 545 nm for 2.1 nm quantum dots is also obtained for the visible emission component, similar to what is reported in literature.[25,31] For quantum-confined ZnO, the widening of the bandgap is expected to result mainly from the upward movement of conduction band states due to the smaller effective mass of the electron than the hole.[12,14,26,32,33] The fact that the energy shift for the visible emission (0.17 eV) is of similar magnitude to that observed for the UV emission (0.15 eV), indicates that for the visible emission, recombination most likely occurs from states close to the conduction band to deep defects in the vicinity of the valence band. This will be discussed in more detail below.

A central issue for applications of the ZnO quantum dots as light emitter is the photoluminescent quantum yield (PLQY). The ZnO quantum dots exhibit both UV and visible light emission. The PLQY of the ZnO quantum dots, measured in ethanol dispersion, at an excitation wavelength of 315 nm, is shown in **Figure 4**. For these measurements, we integrated over the entirety of the emission, including both the UV and visible photoluminescence in the PLQY calculation. There are three remarkable results: first, a peak PLQY of 60% is achieved for the air-exposed 2.1 nm quantum dots, which is to our knowledge the highest value reported on any kind of compound semiconductor nanoparticles synthesized in the gas phase. Second, a clear dependence on air exposure of the ethanol dispersion is obtained: as-produced ZnO quantum dots dispersed in ethanol exhibit PLQYs of 9% and 42% for 3.4 nm and 2.1 nm quantum dots, respectively. After exposure to ambient air for one day, PLQYs from those samples increased to 12% and 60%. Third, the PLQY of the ZnO quantum dots increases as size decreases, for both fresh and air-exposed samples. A similar

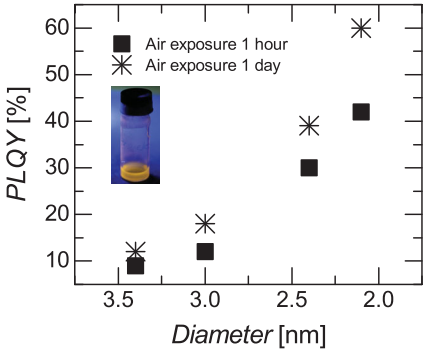

Figure 4. Photoluminescence quantum yield of the ZnO quantum dots with different sizes dispersed in ethanol, measured after air exposure of the dispersion for 1 hour and 1 day. The inset shows a dispersion of particles with a diameter of 2.1 nm in ethanol under UV excitation at 360 nm.

size dependence of the quantum yield—albeit with significantly lower absolute values—was reported for small ZnO quantum dots synthesized using a wet chemical approach.[11] The increase of the PLQY with decreasing quantum dot size is opposite to what is obtained for many other quantum dot materials, for example, for Si and CdSe quantum dots, where the PLQY significantly decreases with smaller size.[34,35] This points to the role of surface states in the luminescence properties of ZnO quantum dots, which may differ in comparison to other materials.

4. Green–Yellow Luminescence Mechanism

The mechanism of the green–yellow luminescence in ZnO—responsible for the high PLQY in our quantum dots—is highly debated. It is likely that there is more than one path for charge carrier recombination in this spectral range and that the importance of each one depends on the relative density of the involved states, which are influenced by the synthesis method and the quantum dot surface conditions.

The charge carrier recombination mechanism leading to the green emission in ZnO is attributed to singly ionized oxygen vacancies by the vast majority of reports in literature.[11,17,25,36–40] The proposed process involves the capture of photogenerated holes in the valence band by surface OH groups that bond to the quantum dots in humid ambient air or in an ethanol dispersion.[17,25,40] The holes, captured by the OH groups, have a finite probability to tunnel back into the crystal to singly ionized oxygen vacancies ($V_O^{\bullet}$), creating a doubly ionized recombination center ($V_O^{\bullet\bullet}$) with an energy level closer to the valence band. A shallow trapped electron may recombine with the captured hole at this center, emitting green light. The tunnelling probability is expected to strongly increase with reduced particle size.[11] This model is consistent with our experimental findings and can explain the higher PLQY in smaller particles, together with the increased ratio of surface to volume for smaller quantum dots and thus the increased availability of oxygen vacancy concentration and OH-groups at the surface.[41,42] It must be noted that there have been recent reports on ZnO quantum dots that show green luminescence without the presence of $V_O^{\bullet}$, which was demonstrated by the missing EPR signal of this paramagnetic state.[43] In addition, aside from oxygen vacancies, there have also been reports that claim oxygen interstitials and anti-sites are responsible for the green emission.[9,39,44] Emission directly involving surface states of OH groups themselves, however, are reported to show lower-energy yellow emission at around 577 nm (2.15 eV).[45,46]

To further uncover the mechanism of the green–yellow luminescence of the plasma-synthesized ZnO quantum dots, PL spectra of the 2.4 nm quantum dots dispersed in ethanol were recorded in nitrogen and in ambient atmosphere under UV illumination. In **Figure 5**a, PL spectra measured under different conditions are shown. The reference (black line) is the PL measurement of the ZnO quantum dots prior to air exposure, which was performed in nitrogen atmosphere. In the reference case, the particles have been exposed to UV light only for several tens of seconds during the measurement. When under continuous UV illumination while still in a nitrogen environment, the green–yellow emission decreases and vanishes almost completely after 4 minutes of exposure. This effect is reversible by exposing the same dispersion to ambient air, where the green–yellow emission reappears and continues to increase on a timescale of several days.

Similar effects of quenching of visible emission by UV exposure have been already discussed in literature.[17,28,30,43,47] It is assumed that after UV excitation and electron-hole pair generation, adsorbed solvent molecules like ethanol act as hole scavengers in an oxidation process. At the same time, adsorbed oxygen, if available, scavenges the electron, which can be consumed in a reduction of free hydrogen ions to dihydrogendioxide.[48] Under aerobic conditions, both reactions can be repeated arbitrarily often because the amount of available solvent and oxygen molecules to be adsorbed is not limited. In that case, visible emission is expected to occur, in agreement with our findings. Under anaerobic conditions, only the solvent adsorption and hole scavenging can be repeated, while adsorbed oxygen cannot be replenished and the electron scavenging process is stopped. This leads to a charge imbalance with excess electrons, which is the widely accepted reason for the quenching of the visible PL under anaerobic conditions.[28,43,49] Earlier reports argue that these excess electrons

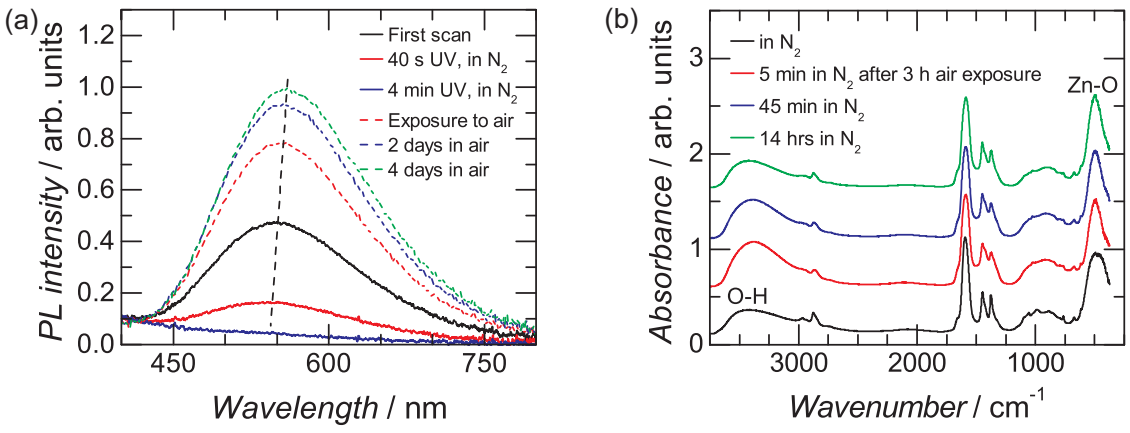

Figure 5. a) PL intensity of the 2.4 nm ZnO quantum dots after exposing to UV light in nitrogen and ambient atmosphere. Dashed black lines act as a guide to the eye indicating the peak emission wavelength shifts. b) FTIR spectra of the 2.4 nm ZnO quantum dots kept under nitrogen atmosphere, and after exposure to air for 3 h and reintroduction of nitrogen for 5 min, 45 min, and 14 h.

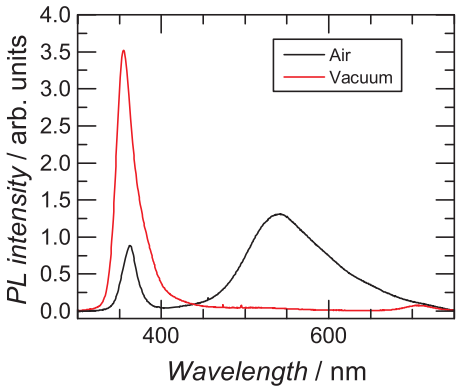

Figure 6. PL intensity of the 2.1 nm ZnO quantum dots in ambient atmosphere and in vacuum (5×10^{-5} mbar), measured at room temperature.

are trapped by the $V_O^{\bullet}$ center, forming oxygen vacancies with two electrons and thus quenching green luminescence,[49] whereas a very recent study concludes that the quenching of the visible emission is related to Auger de-excitation of the emissive state by the excess electrons.[43]

Interestingly, a blue shift of the visible emission is observed under UV excitation, while a redshift is obtained after exposure to air, as indicated by the dashed line in Figure 5a. The findings reported in literature regarding PL shift following UV irradiation are quite diverse, with some groups seeing little or no energy shift,[28,43] and others finding a blue shift similar to our results.[17,30] Although the definite reason for the energy shift of the visible emission observed in our experiment is still unclear, one hypothesis is that the blue shift is related to the charging of the quantum dots or UV-induced breaking/desorption of certain surface species (e.g., OH-groups), by which higher-energy emissions from different kinds of surface defects could become dominant. Supporting the surface desorption/adsorption hypothesis is the observation that under UV illumination, the visible emission is quenched, while after exposure to air, the visible emission is enhanced.

To elucidate more details about the mechanism leading to the strong green–yellow emission from the air-exposed ZnO quantum dots presented here and to reveal possible connections with the surface chemistry, we performed FTIR measurements under different atmospheres (Figure 5b). In particular, we closely examined the OH stretching vibration, which is a broad FTIR feature near 3400 cm^{-1}. The ZnO quantum dots that had never been exposed to air and were stored in nitrogen show the smallest OH bonding signal. After being in contact with ambient air for 3 h, the quantum dots show an increase in the OH bonding peak, while a subsequent storage in N_2 atmosphere reverts this effect again: after 45 min, a decrease in signal intensity is noticeable and after 14 h the intensity of the OH bonding peak is almost the same as for the particles before they were exposed to air. Based on these results, exposure to air readily increases the number of OH bonds on the surface of the ZnO quantum dots. This finding is qualitatively consistent with the hypothesis that OH groups act as surface traps for photogenerated charge carriers, enhancing visible emission.

To further discuss the importance of OH-groups on the visible emission, PL studies of the ZnO quantum dots under high vacuum (HV) conditions have been performed. The measurement temperature was 300 K and during the measurements, the vacuum level was 5×10^{-5} mbar. As can be seen in **Figure 6**, no green–yellow emission signal is observed in HV, whereas the near bandgap emission significantly increases by factor of about 3. In fact, vacuum is expected to desorb surface oxygen-containing species, such as OH groups.[50] Thus, we attribute the reduction in visible PL and the increasing intensity of UV emission under HV conditions to the absence of OH-groups according to the mechanism discussed above. This consideration is also consistent with our FTIR measurements.

5. Conclusions

In summary, we have synthesized quantum dots of the compound semiconductor ZnO using a nonthermal plasma reactor, which is a unique and flexible synthesis tool that provides control over quantum dot size and chemistry. The as-deposited ZnO quantum dots can be synthesized in a size range sufficiently small to demonstrate quantum size effects, and exhibit PLQYs as high as 60% in the visible part of the spectrum. Further, we investigated the effect of size and atmosphere on the luminescence properties of the ZnO quantum dots. Irradiation of the quantum dots with UV light suppresses the visible emission efficiency, while, air exposure enhances the visible emission. These observations, in combination with the FTIR measurements of the ZnO quantum dots in various atmospheres, demonstrate the importance of surface OH-groups for high visible-range quantum yield, which is consistent with the commonly accepted role of surface OH-groups in the visible emission mechanism. The high quantum yields achieved in this work add to the promise of these ZnO quantum dots in light emitting applications.

6. Experimental Section

The PLQY is defined as the ratio of emitted photons to absorbed excitation photons. To determine it, an absolute method was used, as described in detail in the literature.[51] Before measurement, the ZnO quantum dots were dispersed in ethanol in a nitrogen-filled glove box and were measured at the same day they were dispersed. A light-emitting diode (Seti UVTOP-315) was used to excite the ZnO quantum dot dispersion in an integrating sphere (Labsphere) and measure the combined transmitted excitation and sample photoluminescence with a fiber spectrometer (Ocean Optics USB 4000) with a free spectral range of 170 to 880 nm. The spectral response of the spectrometer has been calibrated with a NIST traceable calibration lamp (Ocean Optics LS-1-CAL). All measurements were repeated three times and averaged to improve accuracy. The PL measurements shown in Figure 5a were performed in this setup as well.

The PL spectra of the ZnO quantum dots presented in Figure 3 were measured with a PTI Quantum Master 4 Fluorometer. For these experiments, the ethanol dispersions of the ZnO quantum dots were prepared in the glove box and then kept in air for one day. FTIR measurements were done in nitrogen-purged glove box using an ALPHA infrared spectrometer (Bruker Optics) in the diffuse reflectance infrared Fourier transform spectroscopy (DRIFTS) mode.

XRD measurements were performed using a Bruker-AXS Microdiffractometer with a 2.2 kW sealed Cu X-ray. The quantum dots had been exposed to air for several hours before the XRD measurement.

HRTEM images were acquired in an FEI Tecnai G2 F30 operating at 300 keV. The quantum dots were deposited directly on a carbon-coated TEM grid inside the reactor. Particles had been exposed to ambient air for one day prior to measurements.

Acknowledgements

J.Y. and U.K. acknowledge support through the Materials Research Science and Engineering Center funded through NSF grant DMR-DMR-0819885. P.F. and G.B. acknowledge the Deutsche Forschungsgemeinschaft through grant DFG-GRK-1240. The authors are grateful to Dr. Rebecca Anthony for carefully proofreading the manuscript.

Received: October 7, 2013
Published online: December 4, 2013

[1] C. Lee, Y. Hui, W. Su, C. Lin, *Appl. Phys. Lett.* **2008**, *92*, 261107.
[2] E. Neshataeva, T. Kümmell, G. Bacher, A. Ebbers, *Appl. Phys. Lett.* **2009**, *94*, 091115.
[3] E. Nannen, T. Kümmell, A. Ebbers, G. Bacher, *Appl. Phys. Express* **2012**, *5*, 035001.
[4] T. Omata, Y. Tani, S. Kobayashi, K. Takahashi, A. Miyanaga, Y. Maeda, S. Otsuka-Yao-Matsuo, *Appl. Phys. Lett.* **2012**, *100*, 061104.
[5] E. Neshataeva, T. Kümmell, G. Bacher, in *Inorganic Nanoparticles: Synthesis, Applications, and Perspectives* (Eds.: C. Altavilla, E. Ciliberto), CRC Press, Boca Raton, FL, **2011**, pp. 109–132.
[6] K. Matsuyama, K. Mishima, T. Kato, K. Irie, K. Mishima, *J. Colloid Interface Sci.* **2012**, *367*, 171.
[7] R.-O. Moussodia, L. Balan, C. Merlin, C. Mustin, R. Schneider, *J. Mater. Chem.* **2010**, *20*, 1147.
[8] X. Tang, E. S. G. Choo, L. Li, J. Ding, J. Xue, *Chem. Mater.* **2010**, *22*, 3383.
[9] Q. Ou, T. Matsuda, M. Mesko, A. Ogino, M. Nagatsu, *Jpn. J. Appl. Phys.* **2008**, *47*, 389.
[10] R. Senger, K. Bajaj, *Phys. Rev. B* **2003**, *68*, 045313.
[11] A. van Dijken, J. Makkinje, A. Meijerink, *J. Lumin.* **2001**, *92*, 323.
[12] N. Wang, Y. Yang, G. Yang, *Nanoscale Res. Lett.* **2011**, *6*, 338.
[13] H.-M. Cheng, K.-F. Lin, H.-C. Hsu, W.-F. Hsieh, *Appl. Phys. Lett.* **2006**, *88*, 261909.
[14] M. Sessolo, H. J. Bolink, H. Brine, H. Prima-Garcia, R. Tena-Zaera, *J. Mater. Chem.* **2012**, *22*, 4916.
[15] S. J. Yang, C. R. Park, *Nanotechnology* **2008**, *19*, 035609.
[16] Y.-S. Fu, X.-W. Du, S. A. Kulinich, J.-S. Qiu, W.-J. Qin, R. Li, J. Sun, J. Liu, *J. Am. Chem. Soc.* **2007**, *129*, 16029.
[17] A. van Dijken, E. A. Meulenkamp, D. Vanmaekelbergh, A. Meijerink, *J. Phys. Chem. B* **2000**, *104*, 1715.
[18] K. Stipan, G. Michael, P. Kress, G. J. Varga, E. Staab, W. Weber, (Evonik Industries AG), *United States Patent US 7,718,261 B2*, **2010**.
[19] H. Kleinwechter, C. Janzen, J. Knipping, H. Wiggers, P. Roth, *J. Mater. Sci.* **2002**, *37*, 4349.
[20] S. Polarz, A. Roy, M. Merz, S. Halm, D. Schröder, L. Schneider, G. Bacher, F. E. Kruis, M. Driess, *Small* **2005**, *1*, 540.
[21] M. Ali, N. Friedenberger, M. Spasova, M. Winterer, *Chem. Vap. Depos.* **2009**, *15*, 192.
[22] L. Mangolini, E. Thimsen, U. Kortshagen, *Nano Lett.* **2005**, *5*, 655.
[23] F. E. Kruis, H. Fissan, A. Peled, *J. Aerosol Sci.* **1998**, *29*, 511.
[24] A. Patterson, *Phys. Rev.* **1939**, *56*, 978.
[25] L. Zhang, L. Yin, C. Wang, N. Lun, Y. Qi, D. Xiang, *J. Phys. Chem. C* **2010**, *114*, 9651.
[26] T. J. Jacobsson, T. Edvinsson, *Inorg. Chem.* **2011**, *50*, 9578.
[27] K.-F. Lin, H.-M. Cheng, H.-C. Hsu, L.-J. Lin, W.-F. Hsieh, *Chem. Phys. Lett.* **2005**, *409*, 208.
[28] O. L. Stroyuk, V. M. Dzhagan, V. V Shvalagin, S. Y. Kuchmiy, *J. Phys. Chem. C* **2010**, *114*, 220.
[29] M. Yin, Y. Gu, I. L. Kuskovsky, T. Andelman, Y. Zhu, G. F. Neumark, S. O'rien, *J. Am. Chem. Soc.* **2004**, *126*, 6206.
[30] S. Yamamoto, *J. Phys. Chem. C* **2011**, *115*, 21635.
[31] E. M. Wong, P. C. Searson, *Appl. Phys. Lett.* **1999**, *74*, 2939.
[32] T. Omata, K. Takahashi, S. Hashimoto, Y. Maeda, K. Nose, S. Otsuka-Yao-Matsuo, K. Kanaori, *J. Colloid Interface Sci.* **2011**, *355*, 274.
[33] G. Kiliani, R. Schneider, D. Litvinov, D. Gerthsen, M. Fonin, U. Rüdiger, A. Leitenstorfer, R. Bratschitsch, *Opt. Express* **2011**, *19*, 1641.
[34] M. L. Mastronardi, F. Maier-Flaig, D. Faulkner, E. J. Henderson, C. Kübel, U. Lemmer, G. A. Ozin, *Nano Lett.* **2012**, *12*, 337.
[35] L. Qian, Y. Zheng, J. Xue, P. H. Holloway, *Nat. Photonics* **2011**, *5*, 543.
[36] M. Ghosh, A. K. Raychaudhuri, *Nanotechnology* **2008**, *19*, 445704.
[37] A. N. Gruzintsev, E. E. Yakimov, *Inorg. Mater.* **2005**, *41*, 725.
[38] A. van Dijken, E. A. Meulenkamp, D. Vanmaekelbergh, A. Meijerink, *J. Lumin.* **2000**, *90*, 123.
[39] L. Irimpan, V. P. N. Nampoori, P. Radhakrishnan, A. Deepthy, B. Krishnan, *J. Appl. Phys.* **2007**, *102*, 063524.
[40] N. S. Norberg, D. R. Gamelin, *J. Phys. Chem. B* **2005**, *109*, 20810.
[41] A. B. Djurišić, W. C. H. Choy, V. A. L. Roy, Y. H. Leung, C. Y. Kwong, K. W. Cheah, T. K. Gundu Rao, W. K. Chan, H. Fei Lui, C. Surya, *Adv. Funct. Mater.* **2004**, *14*, 856.
[42] J. Liu, P. Gao, W. Mai, C. Lao, Z. L. Wang, R. Tummala, *Appl. Phys. Lett.* **2006**, *89*, 063125.
[43] A. W. Cohn, N. Janßen, J. M. Mayer, D. R. Gamelin, *J. Phys. Chem. C* **2012**, *116*, 20633.
[44] B. Lin, Z. Fu, Y. Jia, *Appl. Phys. Lett.* **2001**, *79*, 943.
[45] A. B. Djurišić, Y. H. Leung, K. H. Tam, Y. F. Hsu, L. Ding, W. K. Ge, Y. C. Zhong, K. S. Wong, W. K. Chan, H. L. Tam, K. W. Cheah, W. M. Kwok, D. L. Phillips, *Nanotechnology* **2007**, *18*, 095702.
[46] K. H. Tam, C. K. Cheung, Y. H. Leung, A. B. Djurisić, C. C. Ling, C. D. Beling, S. Fung, W. M. Kwok, W. K. Chan, D. L. Phillips, L. Ding, W. K. Ge, *J. Phys. Chem. B* **2006**, *110*, 20865.
[47] V. Subramanian, E. E. Wolf, P. V Kamat, *J. Phys. Chem. B* **2003**, *107*, 7479.
[48] D. S. Bohle, C. J. Spina, *J. Am. Chem. Soc.* **2009**, *131*, 4397.
[49] A. van Dijken, E. A. Meulenkamp, D. Vanmaekelbergh, A. Meijerink, *J. Phys. Chem. B* **2000**, *104*, 4355.
[50] A. Sharma, B. P. Singh, S. Dhar, A. Gondorf, M. Spasova, *Surf. Sci.* **2012**, *606*, L13.
[51] D. Jurbergs, E. Rogojina, L. Mangolini, U. Kortshagen, *Appl. Phys. Lett.* **2006**, *88*, 233116.